A quantum dot–lucigenin probe for Cl^-†

Maria Jose Ruedas-Rama and Elizabeth A. H. Hall*

Received 28th January 2008, Accepted 9th June 2008
First published as an Advance Article on the web 1st August 2008
DOI: 10.1039/b801507d

In this work, the first chloride ion sensor based on QD–lucigenin nanoparticles is reported. The mechanism uses the ability of semiconductor QDs to engage in short range exchange processes, leading to fluorescence changes. An acridinium dication (lucigenin) which is an electron acceptor, was self-assembled on the surface of negative charged QDs (capped with mercaptopropionic acid). Mutual quenching of the lucigenin and QD were observed. From a sphere of action, Perrin-type model, exchange was estimated to occur over a range of the order of 2 nm. The possibility of spin–orbit coupling (SOC) or electron transfer between the QD and the lucigenin dication (Luc^{2+}) is discussed. The radical cation $Luc^{+\bullet}$ was not identified, but electron transfer from the QD conduction band to the Luc^{2+}, then electron transfer back, from the $Luc^{+\bullet}$ to the QD valence band, could lead to mutual quenching, without build up of $Luc^{+\bullet}$. SOC between the QD and lucigenin, with or without charge transfer being involved, can also account for the results obtained. Lucigenin is also a chloride-sensitive indicator dye, with a sensing mechanism based on SOC. In the QD–MPA–lucigenin conjugate luminescence is restored by adding chloride ion. Thus, the presence of chloride is transduced into an enhancement of the luminescence of QDs. Using this operating principle, a chloride ion sensor based on CdSe–ZnS core–shell QD nanoparticles, showed a very good linearity in the range 1–250 mM, with a detection limit 0.29 mM and a RSD of 2.5% ($n = 10$). In a study of interferences, the chloride sensitive QDs showed good selectivity to most of the other anions tested. The versatility of the system was also demonstrated in terms of fluorescent emission wavelength, which could be selected across a wide range through choice of QDs. Examples are shown for $\lambda_{max} = 500$, 540 and 620 nm. The results from samples mimicking physiological conditions suggested very good applicability in the determination of chloride ion in physiological samples.

Introduction

Many optical microsphere[1,2] or nanosphere[3–5] systems for ion-sensing require cation exchange and/or co-extraction of anions and protons into the bulk of a polymer containing an ion-selective carrier and a lipophilic pH chromophore or fluorophore indicator.[6–8] However, low photostability of the fluorophores employed can be a factor limiting the performance of these systems. In contrast, colloidal semiconductor nanocrystals or quantum dots (QDs) act as highly efficient and photostable fluorophores with a relatively long fluorescent lifetime (dependent on size), better chemical and photoluminescence stabilities than the conventional organic fluorophores, and resistance to photobleaching.[9,10]

In direct analogy with the classical fluorophore/ionophore systems cited above, the determination of ions of physiological interest has been shown, by using QDs as a labelling component[11] within a polymer particle. However, this may not be the best/only way to exploit the photoluminescence properties of QDs, which arise from the recombination of the exciton. Some chemical sensing systems based on QDs have been conceived, using fluorescence changes induced by direct physical adsorption or chelating of ions[12–14] on the surface of QDs activated by the exchanged ligand or by direct reaction with surface modified QDs.[15,16] The recombination of charge carriers either before they are trapped (band gap recombination) or while they are in very shallow traps (near band gap recombination), should be influenced by changes of surface charge or ligand components of QDs that alter the core electron–hole recombination and consequently the luminescence. However, many of the responses still cannot be fully predicted, with mechanistic understanding often speculative, contradictory or missing in detail.

Nevertheless, the ability to control electron transfer to/from the QD and influence the non-radiative recombination of exited electrons in the conduction band and holes (h^+) in the valence band, through analyte-specific interactions at the surface should offer considerable analytical capability. In this context, the use of QD–electron donor/acceptor systems is potentially very promising, since electron transfer can alter the luminescence of QD nanoparticles. Electron transfer between semiconductor particles and organic molecules was first carried out with TiO_2 nanocrystals to realize photovoltaic devices,[17,18] but the application of such charge transfer processes with CdSe and CdSe–ZnS quantum dots are now also being investigated.[19–21] Moreover, some literature data demonstrate that QDs can

Institute of Biotechnology, University of Cambridge, Tennis Court Road, Cambridge, UK CB2 1QT. E-mail: lisa.hall@biotech.cam.ac.uk; Fax: +44 1223 334161; Tel: +44 1223 334149

† Electronic supplementary information (ESI) available: Chloride response of QD–MPA–lucigenin and QD–DHLA–lucigenin conjugates. See DOI: 10.1039/b801507d

also efficiently transfer electrons to complementary acceptors under excitation, with an effective quenching of luminescence. Although the mechanisms remain to be fully elucidated,[22–26] this idea needs to be further explored in the context of its potential extension for use in analytical systems.

For example, looking at the underlying process, some dication derivatives have been shown to be electron acceptors for excited QDs,[23,24] quenching their luminescence mainly because it prevents the radiative recombination. Yildiz and collaborators proposed a supramolecular association of complementary receptor–substrate pairs leading to an enhancement of the luminescence of QDs.[24] Methyl viologen for example, acts as electron-acceptor-quencher, suppressing the emission of QDs when adsorbed on the surface, on the basis of photoinduced electron transfer. In this instance, the process gains analytical usefulness, since the quenching can be reversed by sequestering and removing the quencher from the surface of the QDs, by addition of a host receptor, *e.g.* cucurbituril. Thus, this principle could be implemented and extended to detect DNA or protein or antigen–antibody interactions. However, an elegant analytical system might be conceived whereby an integrated electron-acceptor-quencher capability of the adsorbed reagent/ligand itself is modulated, during the analytical step, without needing sequestration or other desorption process to change the luminescence of the QDs.

On this foundation, we want to explore how QD–redox pairs could provide a basis for the generation of other analytical systems. The work presented herein examines the QD–acridinium dication interaction using lucigenin (bis-*N*-methylacridinium) as a model to provide the basis for a directly responsive ion-selective QD (I-QD). Luciginin is a chloride-sensitive indicator dye, so that a dynamic chloride dependent quenching mechanism would normally be anticipated in solution, based on the photophysical process between the quencher and photo-excited lucigenin.[27–29]

Experimental

Materials

Quantum dots CdSe–ZnS core shell with maximum emission at 490, 540 and 620 nm were purchased from Evident Technologies. The surfactant capping the QDs was a long chain (16 C) amine with some tri-*n*-octylphosphine/tri-*n*-octylphosphine oxide (TOP/TOPO) present. Bis-*N*-methylacridinium nitrate (lucigenin), (±)-α-lipoic acid, and dimethylformamide were obtained from Aldrich. All inorganic salts including phosphate buffers were of analytical grade and used as obtained from Aldrich. 3-Mercaptopropionic acid, potassium *tert*-butoxide, and citric acid monohydrate were purchased from Fluka. All standard chemical solutions were protected from sunlight and kept at about 5 °C in a refrigerator. Standard salt solutions and HCl and NaOH solutions were prepared in milli-Q water.

Synthesis of water soluble MPA and HDLA capped CdSe–ZnS nanoparticles

The lipophilic hexadecylamine-capped QDs were modified by 3-mercaptopropionic acid to achieve water solubility with preservation of high luminescence quantum yield. Two procedures were employed for the surface–ligand exchange based on previous reports.[30–34] In brief, to achieve mercaptopropionic acid (MPA) capped QDs, 1 mL of QDs (Evident Technologies: hexadecylamine as ligand) dissolved in toluene was left to react overnight with 1 ml of MPA, protected from light.[32] After the ligand exchange, the particles were transferred to an aqueous phase by adding 1 M NaOH solution (2 mL) and shaking. The two phase mixture was separated, and the water-soluble CdSe–ZnS QD nanoparticles were separated from the excess of MPA by precipitation of the particles with acetone and centrifugation, followed by the re-dissolution of the MPA capped QDs in milli-Q water.

For dihydrolipoic acid (DHLA) capped water soluble QDs, DHLA was prepared from lipoic acid as previously described in the literature.[33] 80 μL of the colourless oil obtained as product was added to the QDs, after the evaporation of the toluene from 1 mL QDs solution used as supplied. The mixture was heated to 70 °C for 2–3 h. After cooling, 1 mL dimethylformamide (DMF) was added to the suspension, and the deprotonation of the terminal carboxylic acid groups was carried out by slowly adding excess potassium *tert*-butoxide.[33,35] The resulting precipitate was sedimented by centrifugation, and the supernatant containing the lipophilic hexadecylamine was discharged. The precipitate was dispersed in water, and reprecipitated with acetone until a transparent and water soluble DHLA capped CdSe–ZnS QDs solution was obtained.

Optimisation of MPA/QDs and QD–MPA/lucigenin ratios

The carboxylic acid-terminated capping groups provide a negative charge surface distribution that can promote direct self-assembly with positively charged compounds such as lucigenin. QDs of this type are expected to form stable QD–MPA–lucigenin conjugates through electrostatic interactions. To obtain water-soluble QDs, with a suitable negatively charged surface to interact with the positively charged lucigenin, different QD : MPA ratios were tested. Using a fixed quantity of commercial QD_{620}, 200 μL (4 nmol), the ligand exchange was carried out with different MPA volumes, from 20 to 200 μL (corresponding to 230 to 2300 μmol, respectively).

After capping exchange,[32] QD_{620}–MPA was precipitated with acetone, centrifuged, and re-dissolved in milli-Q water. Every QD_{620}–MPA batch was conjugated with the same concentration of lucigenin, and the chloride response was tested.

To study the effect and optimise the quantity of lucigenin conjugated to the surface of QDs, different volumes of a lucigenin solution in water were added to a fixed quantity of QD_{620}–MPA (0.7 nmol). After 30 min interaction, QD_{620}–MPA–lucigenin conjugates were precipitated with acetone and centrifuged. The supernatant was removed and the orange QD residue was re-dissolved in milli-Q water. The amount of lucigenin tested to measure the chloride response ranged from 2.44–39.16 nmol.

Preparation of the QD–MPA–lucigenin conjugates

The proposed chloride ion sensing QDs developed here are based on MPA capped CdSe–ZnS core–shell QDs and lucigenin conjugate, but also can be obtained with DHLA capped QDs (Fig. SI-1†). Lucigenin was coupled to QD–MPA (or QD–DHLA) through electrostatic interaction between negatively charged QD surfaces and the positively charged nitrogens of

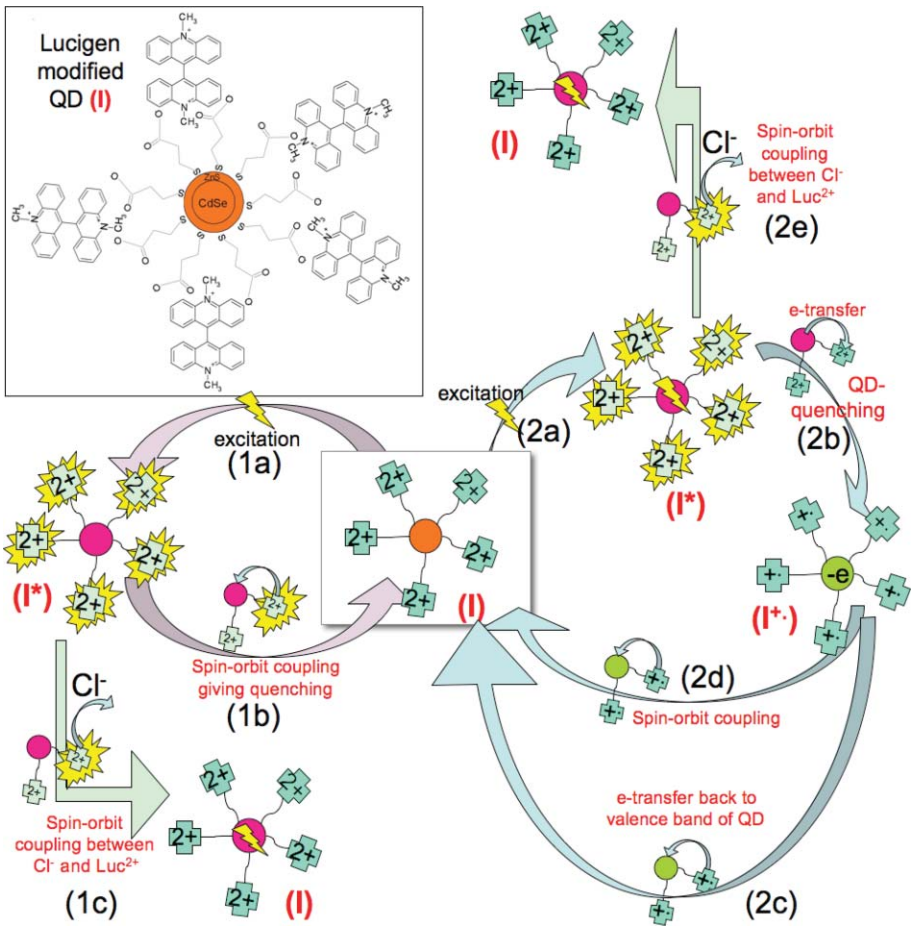

Fig. 1 Scheme of the QD_{620}–MPA–lucigenin (I) conjugate after self-assembly by electrostatic interactions. *Pathway 1*: (a) excitation, (b) quenching *via* spin–orbit-coupling (SOC) and (c) competition by Cl^- for SOC with lucigenin. *Pathway 2*: (a) excitation, (b) QD quenching (and thus bleaching) *via* electron transfer between lucigenin and the QD, (c) electron transfer from lucigenin to QD thus reversing bleaching, (d) SOC and (e) competition by Cl^- for SOC with lucigenin.

the acridinium derivative (see scheme in Fig. 1). Very stable structures can be formed through a self-assembly strategy.[35–37] The data reported herein focuses on the QD–MPA derivative but for comparison of the chloride response of these two conjugates see the ESI.† The conjugate was prepared by mixing the MPA capped QDs and lucigenin in milli-Q water. Approximately 100 μL of lucigenin solution of 50 μg ml^{-1} (~9.8 nmol) were added into 200 μL MPA–QDs solution (~0.7 nmol QDs in water) and allowed to self-assemble by electrostatic interactions for 15 min at room temperature. Separation/isolation of the QDs was performed after self-assembly, to remove them from any free lucigenin that remained in solution. This was required to ensure that the chloride response occurred just with immobilised lucigenin on the surface of QD nanoparticles. Thus, after interaction, QD–MPA–lucigenin conjugates were precipitated with acetone and centrifuged. The supernatant was removed and the residue re-dissolved in milli-Q water. QD–MPA–lucigenin conjugates were re-dissolved in milli-Q water.

However, in line with other reports in the literature, reproducibility between different batches of QDs from the same supplier, can make full quantitative evaluation difficult and each batch must presently be calibrated independently. The interfacial environment of the lipophilic QDs as supplied, can have a significant effect on the MPA derivatisation. This will influence the properties of the resultant water soluble QDs and their ability to bind with lucigenin *via* electrostatic interactions since the ionization equilibria of the surface will be affected. A wide range of interfacial carboxy systems including monolayers,[38] dendrimers[39] and latex particles[40] give pK_a shifts over several orders of magnitude. Although short-chain carboxylic acids have a solution phase pK_a value of approximately 4.8,[41] increases in interchain packing density for alkanoic acids, are proposed to act to stabilize the protonated form through formation of adjacent dimeric species, thus increasing the apparent pK_a up to 10.0.[42,43] In addition, electrostatic interactions between spatially confined carboxylic acid groups in organized assemblies destabilize the carboxylate anion due to the coulombic repulsion. The 'quality' of the MPA derivatisation will thus have an impact on the interaction with the acridinium dication.

In view of the variability in the supplied QD batch, influencing the 'characteristic' of the QD–MPA product, the batch is identified according to the QD quenching obtained at maximum lucigenin binding capacity. For example, in *Batch A* at optimised MPA modification, increasing the quantity of lucigenin up to 9.79 nmol, resulted in quenching of the QDs emission at 620 nm. Higher quantity of lucigenin did not significantly increase the

quenching (Fig. 2a), but increased the lucigenin fluorescence measured at 505 nm and the appearance of a yellow supernatant after centrifugation of the luciginin modified QDs indicated an excess of lucigenin at these higher concentrations (a transparent supernatant was seen when a quantity of lucigenin below 9.79 nmol was used). In conclusion, in this batch, 9.79 nmol is the maximum lucigenin concentration and results in 90–95% quenching, which corresponds to a molar ratio QD : lucigenin of 1 : 14. In contrast, in *Batch B* the same quantity of lucigenin (9.79 nmol) only produced 60–65% quenching, but higher lucigenin concentration did not increase the quantity of lucigenin attached, suggesting that the negative packing density on the surface of QD–MPA was lower, producing less electrostatic interactions with the dication lucigenin. All experiments here were performed with QDs from *Batch A*.

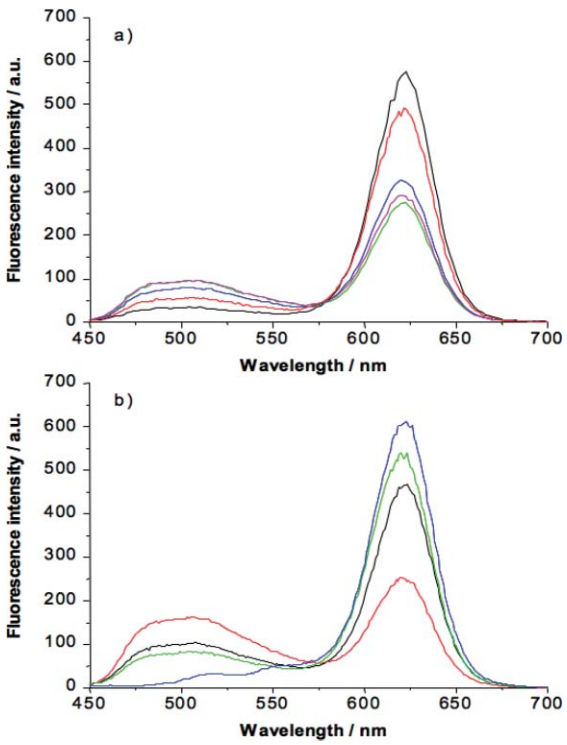

Fig. 2 (a) Emission spectra of QD_{620}–MPA–lucigenin conjugates after attachment different lucigenin amounts: 2.44 nmol (black), 4.89 nmol (red), 9.79 nmol (blue), 19.58 nmol (pink), and 39.16 nmol (green). (b) Emission spectra of different batches QD_{620}–MPA with different MPA mol on the surface after addition lucigenin (9.79 nmol). MPA quantity added to the QDs during the ligand exchange: 5.7×10^4 mol (blue), 2.8×10^5 mol (green), 4.3×10^5 mol (black), and 5.7×10^5 mol (red).

Effect of pH and ionic strength in QD–MPA–lucigenin conjugates

40 μL QD_{620}–MPA–lucigenin conjugates were exposed to 120 μL chloride solutions buffered with phosphate buffer at different pH and different concentrations. The response towards chloride was evaluated in all those media and the linear response plot was calculated and compared. Titrations of QD_{620}–MPA–lucigenin and QD_{620}–MPA with NaOH and H_2SO_4 or H_3PO_4 were also carried out to test the effect of the pH in the luminescence of QDs.

Chloride calibration of the QD–MPA–lucigenin conjugates

Calibration was performed in triplicate. 120 μL of chloride ion stock solutions (ranged 0.1–500 mM) in 50 mM phosphate buffer at pH 7 were added to 40 μL of QD_{620}–MPA–lucigenin conjugate and placed in the quartz microcell for fluorescence scanning. Because of the wide chloride ion response range, the data are presented on a logarithmic scale. The data, corresponding to the average of three determinations, were fitted by standard least-squares treatment and the calibration line was calculated.

Spectrofluorimetric measurements of QD–MPA–lucigenin conjugate

In all experiments, sets of samples were prepared by adding 120 μL of chloride ion stock solutions in phosphate buffer 50 mM pH 7 into 40 μL of QD–MPA–lucigenin conjugate solution (QD : lucigenin molar ratio, 1 : 14). These samples were placed in a quartz microcell (Starna) with a light path length of 10 mm (160 μL inner volume) and the emission spectrum of each sample was measured using a Cary-Eclipse Fluorescence Spectrofluorimeter (Varian). The spectrofluorimeter was equipped with a xenon discharge lamp (75 kV), Czerny–Turner monochromators, two detectors (sample and internal reference), and an R-928 photomultiplier tube with manual or automatic voltage controlled using the Cary-Eclipse software. Instrument excitation and emission slits were set at 5 and 10 nm, respectively, and the scan rate of the monochromators was 600 nm min^{-1}. All samples were illuminated under an excitation wavelength of 400 nm and the emission was scanned from 450 to 700 nm, while the detector voltage was maintained between 550 and 600 V. To study response time, emission intensity was measured as a function of time, and CdSe–ZnS nanoparticle suspensions were scanned every 2 min, until no further change had occurred.

For the determination of chloride ions in simulated physiological samples, 120 μL samples were added into 40 μL of QD_{620}–MPA–lucigenin conjugate solution and spectra were recorded. The samples were taken from a commercial solution Dulbecco's Modified Eagle's Medium (DMEM D-6171, Sigma) and dilutions of this solution prepared in a phosphate buffer at pH 7. This commercial solution, employed for culturing embryonic cells, was used to mimic intracellular conditions. It contains very high concentration of most of the cellular components: inorganic salts, amino acids, vitamins, glucose and other intracellular components.

Results and discussion

QD–lucigenin complex formation

Lucigenin is an acridine fluorophore with high photostability and high fluorescence quantum yield. The acridinium dication interacts electrostatically with the negative charged surface of QD–MPA nanoparticles. Stable QD–MPA–lucigenin conjugates could be formed with different QD : MPA ratios (with a stoichiometric excess between $50–500 \times 10^3$) for the lipophilic-capped QD_{620} (4 nmol) as supplied. The degree of quenching was influenced both by the MPA surface ligand density and the lucigenin concentration. Below 3×10^5 mol of MPA added

to the QDs for the ligand exchange step, no attachment of lucigenin was detected (Fig. 2b), probably suggesting insufficient carboxylic groups on the surface of the QDs, to produce the required interaction with lucigenin. Increasing the ratio of MPA gave successful immobilisation of lucigenin; the resultant QD–MPA was a water soluble QD with a measured pK_a of 6.5 (see later).

The QD–lucigenin complex in the reaction solution showed quenching of the QD luminescence and a small emission band at 505 nm (the maximum emission of free lucigenin, Fig. 2a). Emission spectra of QD_{620}–MPA, lucigenin, and the QD_{620}–MPA–lucigenin conjugate (before and after purification by centrifugation) at the same concentrations were compared under the same working conditions, and a quenching-maximum of luminescence of around 90–95% could be achieved by lucigenin from a 50 mM solution (Fig. 3a). The emission intensity of lucigenin (at 505 nm) and QDs (at 620 nm for QD : lucigenin of 1 : 14) before and after purification and isolation by centrifugation were very similar, which suggests that little/no lucigenin was left in the supernatant. Thus, the attachment on the surface of all lucigenin added was efficient at the concentrations used. Only a small shift of the maximum emission, from 622 nm for QD_{620}–MPA to 620 nm for QD_{620}–MPA–lucigenin was observed. Similar QD–lucigenin ionic conjugates, tested using three different populations of CdSe–ZnS core–shell QDs, all showed mutual fluorescence quenching (Fig. 4), so the quenching mechanism is not dependent on the QD band gap in this range.

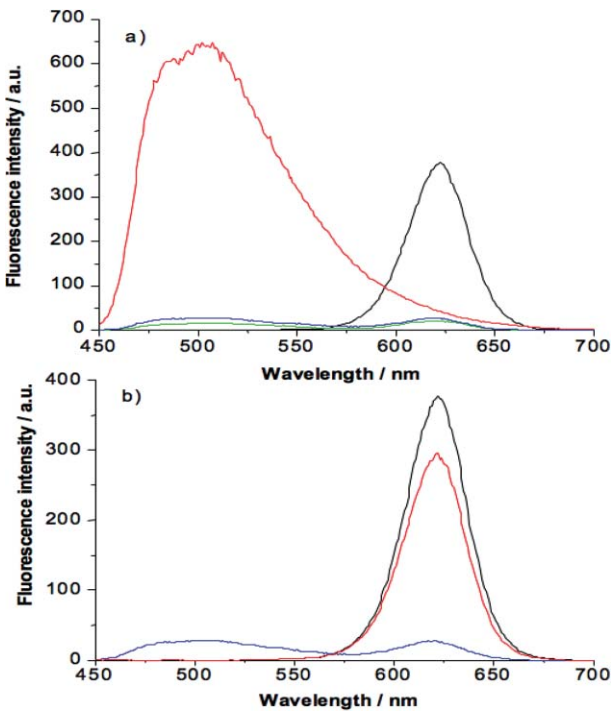

Fig. 3 (a) Emission spectra of separated QD_{620}–MPA (black), lucigenin (red), and QD_{620}–MPA–lucigenin conjugate before (green) and after (blue) purification by precipitation with acetone and centrifugation. All components are at the same concentration in all cases. (b) Emission spectra of QD_{620}–MPA before exposure to lucigenin (black), QD_{620}–MPA–lucigenin conjugate (blue), and QD_{620}–MPA–lucigenin conjugate after addition 2 M KCl (red). In all cases $\lambda_{ex} = 400$ nm.

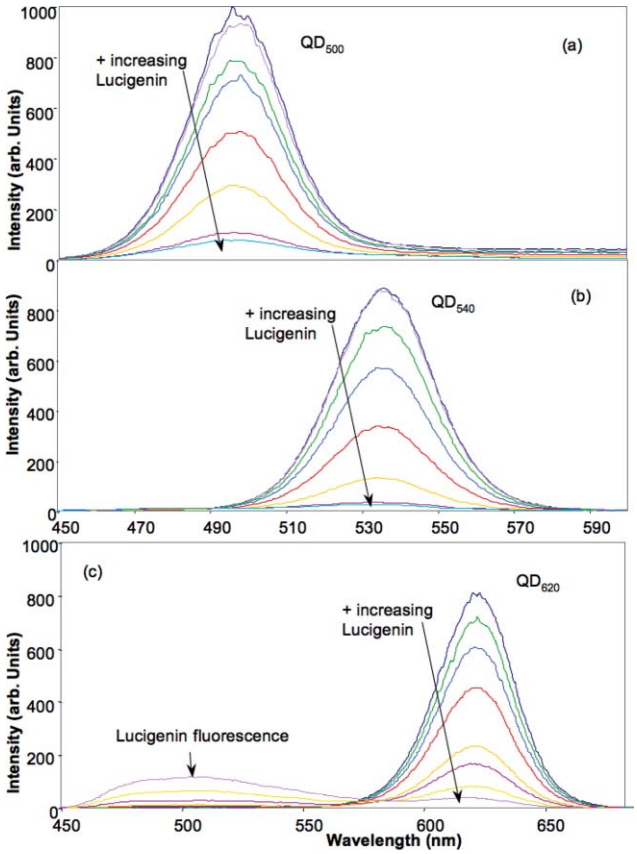

Fig. 4 QD–MPA treated with different concentrations of lucigenin (0–100 mg L^{-1}). Three populations of QDs shown with emission 500 nm, 540 nm and 620 nm.

Response mechanism

The analysis of deviations from Stern–Volmer plots for dynamic fluorescence quenching is an effective way to explore the quenching mechanism. Representative plots are shown for the QD_{620}–lucigenin ($\lambda_{max} = 620$ nm, diameter 5.4 nm) and compared with data for two other populations of quantum dots (λ_{max} = 500, 540 nm; 1.9, 2.4 in diameter respectively) in Fig. 5a. The quenching of the QD excited state may be by collision with a quencher (the dynamic mechanism) or by a static mechanism arising from charge transfer (or electron tunnelling) or the overlap of molecular orbitals. As expected for this immobilised rather than dynamic system, the plots are clearly non-linear. Such a positive deviation can arise in several different models, including static quenching mechanisms and where distance dependent quenching is involved. For example, the non-linear quenching associated with semiconductor nanoparticles,[44] has the same characteristic shape in the Stern–Volmer plot as seen here. A simple Perrin model where quenching of the excited state occurs only within a sphere of action was proposed in this instance, according to:

$$\frac{I_0}{I} = e^{\alpha[\text{lucigenin}]}$$

($\alpha = N_A V$, where N_A is Avogadro's number and V the quenching or 'action' volume). From this relationship a plot of $\ln I_0/I$ *vs.*

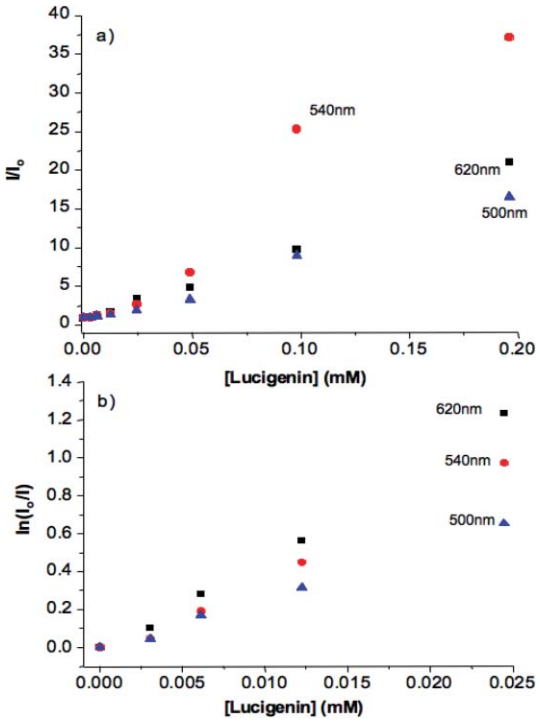

Fig. 5 Plots showing fits to (a) Stern–Volmer quenching and (b) Perrin model sphere of action quenching of QD_{500}–MPA (▲), QD_{540}–MPA (●), and QD_{620}–MPA (■) upon addition lucigenin.

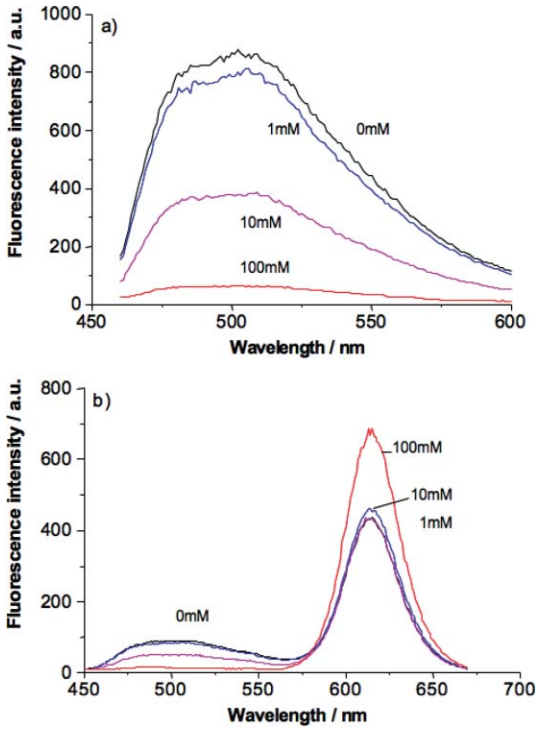

Fig. 6 Emission spectra of (a) lucigenin and (b) QD_{620}–MPA–lucigenin, after addition different concentrations of TEA: black (0 mM); blue (1 mM); pink (10 mM); red (100 mM).

[lucigenin] will reveal V and hence the radius (r) of the sphere of action can be calculated.

In all cases the QD–lucigenin produces 50% quenching efficiency at or below 25 μM lucigenin concentration. Above this concentration the assembly of lucigenin from solution on the QD surface is probably modulated by the already partially occupied surface, so that the $\ln I_0/I$ *vs.* [lucigenin] shows negative deviation. Using the simple Perrin model (Fig. 5b), the sphere of action radii, calculated from the gradient of the plot of $\ln I_0/I$ *vs.* [lucigenin] for lucigenin concentrations below 25 μM are similar for all three QD populations ($r = 2.1$, 2.5 and 2.7 nm respectively for QDs of 500 nm, 540 nm and 620 nm). The value of this action radius defines how far out from the QD (or the lucigenin) the quenching can take place, so it gives some indication of the type of quenching mechanism. These small values suggest contact distances and thus short-range quenching mechanisms.

Acridinium dications have previously been reported to be quenched by CdSe–ZnS QDs[23,24] as a result of an electron transfer mechanism, mainly because this would prevent the radiative recombination, but more precise evidence for this particular mechanism was not presented in these previous discussions. More than one possibility exists to account for such a mutual quenching mechanism.

The lucigenin (bis-*N*-methylacridium) dication (Luc^{2+}) is readily reduced by certain compounds to the radical cation, $Luc^{+\bullet}$. Evidence for a charge transfer mechanism with lucigenin is seen, for example, in its reaction with triethanol amine (TEA), a mild electron donor, which reacts with lucigenin to quench the fluorescence (Fig. 6a), probably as a result of formation of the radical cation ($Luc^{+\bullet}$). QDs have also been demonstrated to be efficient exciton donors with various organic dyes,[45] so that precedent for such a charge transfer in the QD–lucigenin complex is evident. In fact in a QD–lucigenin complex (Fig. 6b), any residual lucigenin fluorescence is quenched in the presence of the TEA electron donor (as would be expected from Fig. 6a), and at very high TEA concentrations the QD fluorescence is partly restored, suggesting that under extreme TEA concentrations, the lucigenin–QD interaction has been disrupted. This could be the result of a competitive electron transfer, which is order(s) of magnitude faster between QD and lucigenin than between TEA and lucigenin, but the result is inconclusive. The nature of the QD–lucigenin exchange may just be a different mechanism to the TEA–lucigenin interaction, so that the idea of a $Luc^{+\bullet}$ state resulting from electron transfer from the QD is not confirmed.

In looking at a TEA/QD/4,4′ bipyridinium-dication combination, Yildiz and Raymo[23] have suggested a QD quenching mechanism involving electron transfer from the QD conduction band to the dication, together with electron transfer from TEA to QD valence band (thereby maintaining the electron population of the QD). Such a pathway doesn't account for direct interaction between TEA and dication, which is clearly evident in our example reported herein (Fig. 6a), so their pathway cannot be extrapolated here.

The $Luc^{+\bullet}$ radical cation is also known to generate chemiluminescence (CL) under alkaline conditions.[46] However, the excited state degradation product, *N*-methylacridone (NMA) with emission maximum ~425 nm, is usually formed in the presence of oxygen:

$$Luc^{2+} + e^- \rightarrow Luc^{+\bullet}$$

$$Luc^{+\bullet} + O_2 \rightarrow Luc^{2+} + O_2^{\bullet -}$$

$$Luc^{+\bullet} + O_2^{\bullet -} \rightarrow Luc(OO) \rightarrow NMA^*$$

so that evidence for this charge transfer process should emerge from the CL at 425 nm and from the subsequent breakdown of the QD–lucigenin complex. Neither of these could be observed. Furthermore, the anticipated coloured $Luc^{+\bullet}$ was not seen and since the CL pathway should also lead to degradation of the QD–lucigenin through irreversible NMA* generation, this would cause QD bleaching. This is not observed. Indeed the QD–lucigenin complex is remarkably stable for 5–6 days and thereafter 'instability' only results from minimal leaching of lucigenin. The latter results in a small increase in the QD emission rather than a QD bleaching.

To investigate the possibility of CL further, QD_{620}–MPA–lucigenin conjugates were exposed to different phosphate–citrate buffer solutions in the range of pH 4–9 to test the effect of pH on the luminescence of QDs. Depending on the propensity of $Luc^{+\bullet}$ to participate in a chemiluminscent degradation pathway, higher pH is likely to increase CL if electron transfer occurs. However, even at high pH, CL could not be detected. No change in the small emission band at 505 nm, corresponding to lucigenin, was noticed for the QD–lucigenin conjugate at different pH, which is analogous to the results obtained for the fluorescence of lucigenin free in solution within the pH range 4–8 in phosphate buffer. However, an enhancement of the emission intensity at 620 nm was detected by increasing the pH in the range 5–8. This 620 nm QD enhancement is probably related to the MPA shell, since experiments made with QD_{620}–MPA in the absence of lucigenin, reached the same enhancement of QD emission by increasing the pH. The fluorescence signal of core–shell QDs is sensitive to the degree of protonation of the carboxylic acid capping the surface.[47] In this instance, the lucigenin-free enhancement increased linearly from pH 5 to 8 and suggested a "pK_a" around 6.5, in the same range as found in the literature for pure MPA, calculated with other methods.

In the presence of lucigenin, this pH response seems to be less reversible. Titration experiments performed for QD_{620}–lucigenin conjugate, showed the gradual enhancement of the luminescence of QDs, when the pH was varied from pH 4 to 9 with NaOH, but in contrast, when the titration was made from pH 9 to acidic pHs with H_2SO_4 or H_3PO_4 the luminescence of QDs at 620 nm remained constant between pH 9–5, and only in more acidic conditions, a decrease of the fluorescence was observed. The same effect was not caused by the ions SO_4^{2-}, PO_4^{3-} or Na^+ as we can see in the interference study shown later. This may be consistent with participation of the CL pathway under certain limited conditions but, we were not able to unambiguously attribute this hysteresis to evidence for or against a charge transfer mechanism between lucigenin and QDs. It may just reflect surface buffering capability.

It is also important to note that CL and/or QD bleaching would be avoided if electron transfer, which occurs from the QD *conduction band* to the Luc^{2+}, producing $Luc^{+\bullet}$, is followed by fast back-electron-transfer from the $Luc^{+\bullet}$ to the QD *valence band*. Both QD and lucigenin would become quenched in this process and, so long as the electron transfer to the valence band was faster than the CL, no photobleaching of the QD would occur. Luc is therefore effectively a shuttle for electron and hole (Fig. 1b). Such a process has been considered in the context of the quenching of fluorescent semiconductor nanoparticles by paramagnetic species.[44]

Alternatively, spin–orbit coupling (SOC) between the QD and Luc excited states (before or after CT) causing triplet state formation should also result in a fluorescence quenching (Fig. 1a) without degradation of the QD–lucigenin. There is also precedence for accelerated intersystem crossing (ISC) induced by the spin–orbit coupling with QDs; *e.g.* certain phthalocyanines in the presence of CdTe QDs, capped with 3-mercaptopropionic acid (MPA) were found to result in long triplet lifetime, high triplet yield and high energy transfer efficiency.[48] Emission from the triplet state is slow, so likely to be quenched by other background processes, resulting in a fluorescence quenching.

Transfer from the lucigenin singlet to triplet state is known and is normally catalysed by halides and pseudo-halides, so that QD catalysed ISC with lucigenin should occur in competition with halides. In the case of this acridinium derivative, a dynamic quenching mechanism, based on collisions between the chloride and photoexcited lucigenin is normally observed in solution, described by the Stern–Volmer equation:[27]

$$\frac{F_0}{F} = 1 + k_q \pi_0 [Q] = 1 + K_{SV}[Q]$$

where F_0 and F are the fluorescence intensities in the absence and presence of quencher, respectively, k_q is the biomolecular quenching constant, τ_0 is the unquenched lifetime, [Q] is the quencher concentration and K_{SV} is the Stern–Volmer quenching constant. In this instance for the QD–lucigenin complex, an increase in QD fluorescence might be expected in the presence of halides, if a competitive QD/Cl^- SOC competition with the lucigenin is established. This reaction could provide a useful basis for a chloride determination assay.

Chloride response

Based on the discussion above, the anticipated response for the Luc–QD in the presence of an ISC catalyst such as a halide should involve the competition between the short range quenching mechanism of the Luc–QD system and the Stern–Volmer quenching of the QD immobilised lucigenin and the free chloride. By using a concentration of lucigenin of 50 mM in the incubation step with the QD at a 1 : 14 ratio with the QD (corresponding to ~95% quenching efficiency between the QD and lucigenin), an enhancement of the emission of the QDs occurred in response to changes in the concentration of chloride (Fig. 1 and Fig. SI.1†). About 80% of maximum emission intensity of CdSe–ZnS QDs (compared with the lucigenin free QDs) was recovered at 2 M chloride ion (Fig. 3b). All QD–lucigenin populations tested showed a similar chloride response, suggesting no QD-size dependence on the basic mechanistic pathway and potentially allowing different emission wavelengths to be selected for [Cl^-] determination depending on the application.

To assess whether the system was suitable for ion-selective sensing, calibration curves were obtained, Fig. 7, inset. The chloride sensitive QDs showed a linear increase in fluorescence per decade change in chloride concentration. This produced analytical fits with good linearity (R^2 = 0.9908) in the range

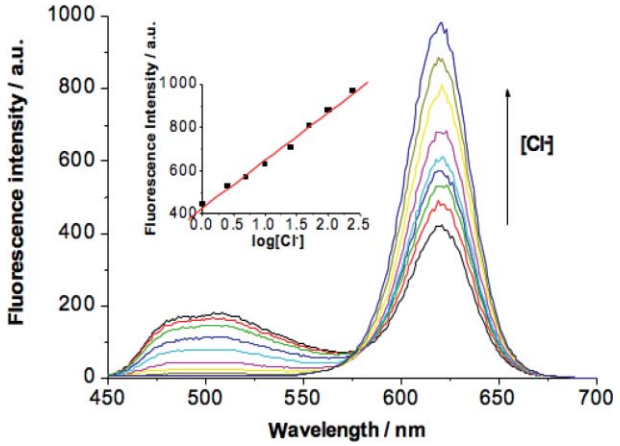

Fig. 7 Emission spectra of QD_{620}–MPA–lucigenin conjugate after addition of different Cl^- concentrations. Inset: Calibration plot at 620 nm.

1–250 mM chloride ion with a reproducible slope ~220 (normalized concentrations at 1 mM, non-dimensional). Linked with the enhancement of the luminescence of QDs (at 620 nm) (Fig. 7), the quenching of the small lucigenin fluorescence band (at 505 nm) was also observed with increasing chloride ion concentration, with I_0/I *vs.* [Cl^-] producing a linear plot consistent with typical Stern–Volmer dynamic collisional quenching. The chloride response was reversible, although as mentioned earlier, slow leaching of electrostatically attached lucigenin over a period of 5–6 days increases the 'background' (zero chloride) fluorescence by up to 20%, so that there is an underlying slope in background fluorescence, which must be taken into account if long-term measurements are required.

It is known that in dynamic quenching of lucigenin the Stern–Volmer constant (K_{SV}), is affected by the ionic strength.[49] In this instance, the chloride enhancement of QD–lucigenin fluorescence was reduced at higher ionic strength, the response towards chloride almost disappearing at very high buffer concentration (phosphate 200 mM, pH 7), whereas the fluorescence emission of the QD–lucigenin conjugate itself was almost unaffected by ionic strength in the range 0.0001–1 M, observing only a very slight increase in emission with increase in concentration of buffer. The slopes of the fluorescence *vs.* log[chloride] response at different buffer concentrations are summarized in Table 1; this effect is usually attributed to the decreased probability of a collisional process because a high concentration of background electrolyte tends to screen the positive charge of the lucigenin moiety.

In line with the underlying pH enhancement of the QDs discussed above, the detection of chloride ion with the QD–lucigenin in 50 mM phosphate buffer solution was seen to increase in sensitivity from pH 4.7 up to pH 7. However, in this instance there was a decrease at more basic pH (8.4) (Table 1). Using this buffer at pH 7, the changes in the emission fluorescence of QDs caused by small changes in pH (in the physiological range) were minimal.

Table 1 Slopes of the chloride ion linear response plot of QD_{620}–MPA–lucigenin conjugate at different pHs and ionic strengths

pH study		Ionic strength study	
Buffer solution	Slope	Buffer solution	Slope
Phosphate 50 mM, pH 4.7	133.6	Phosphate 10 mM, pH 7	231.3
Phosphate 50 mM, pH 5.8	199.3	Phosphate 50 mM, pH 7	217.4
Phosphate 50 mM, pH 7.0	217.4	Phosphate 100 mM, pH 7	46.7
Phosphate 50 mM, pH 8.2	89.6	Phosphate 200 mM, pH 7	—

Repeatability of the proposed chloride sensitive QDs was also checked and established for ten independent analyses. 40 μL of QD_{620}–MPA–lucigenin conjugate, acting Cl^-–nanosensor, were exposed to ten aliquots of 120 μL of 50 mM chloride ion solution buffered with 50 mM phosphate buffer at pH 7. The relative standard deviation (RSD) of the response of these QD-based nanosensors was 2.5%, indicating very good repeatability. The detection limit was 0.29 mM, estimated as the concentration of analyte which produced an analytical signal equal to three times the standard deviation of the background fluorescence.[50] The quantification limit[51] ($K = 10$) was also evaluated, being 0.98 mM.

Response time and selectivity of the proposed chloride sensitive QDs

The response time for the QD_{620}–MPA–lucigenin conjugate to changes in chloride ion concentration, was less than 3 min (see Materials and methods: scan update time was 2 min and >90% response occurred within the second scan). This is consistent with diffusion of chloride ion in the solution to the surface of the QD (*i.e.* no matrix diffusion or phase partitioning) and the dynamic lucigenin quenching mechanism described by the Stern–Volmer plot, producing the quenching of the fluorescence of lucigenin in competition with electron transfer or SOC with the QDs. (Diffusion of Cl^- in solution is 6.4×10^{-8}–12.4×10^{-8} $cm^2\ s^{-1}$ compared with $<10^{-12}$ $cm^2\ s^{-1}$ within polymers and many other hydrocarbon or dendritic matrices. Diffusion of Cl^- within the QD matrix as part of the response mechanism would thus increase the response time). Moreover, the luminescence signal was very stable, even after 30 min, so that photobleaching was not an issue in the measurement.

As expected, the selectivity of the QD_{620}–MPA–lucigenin conjugate towards chloride ion depends of the selectivity of lucigenin. Based on the discussion of the mechanism, it would be expected that the selectivity would be directed to halides and pseudohalides. In the range 0.0001–1 M fluorescence of QDs in the conjugate is not markedly affected by PO_4^{3-}, HCO_3^-, NO_3^- and SO_4^{2-}, because these ions did not compete for quenching of lucigenin (Fig. 8). This is in very good agreement with selectivity data for lucigenin in solution and reported by others,[29] and for lucigenin immobilised onto polymers,[27] for the same foreign ions. Only at concentrations higher than 0.5 M, a weak quenching of lucigenin was detected, producing a small enhancement in the luminescence of QDs. However, as seen above, ion concentration *per se* can alter the sensitivity of the chloride response at this high concentration.

Other halides such as Br^- and I^- showed a pronounced effect on the fluorescence of lucigenin, and therefore, also in the luminescence of QDs (Fig. 8). The very effective quenching by Br^- and I^- has been attributed to the SOC interaction between excited lucigenin and these ions, due to the much lower ionization potential of the higher halides. Fortunately, the expected intracellular biological concentrations of chloride ion

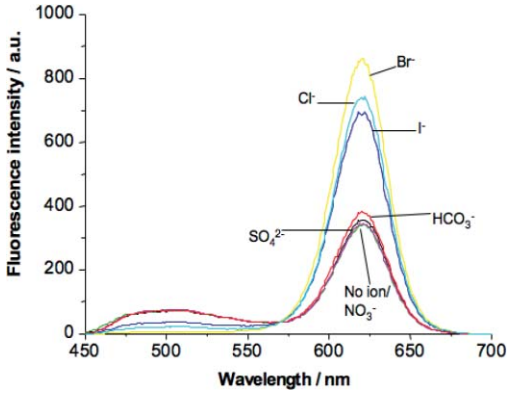

Fig. 8 Emission spectra of QD_{620}–MPA–lucigenin conjugate after addition 100 mM of different foreign ions: No ion (pink), Cl^- (cyan), NO_3^- (green), SO_4^{2-} (black), HCO_3^- (red), I^- (blue), and Br^- (yellow).

(5–15 mM) are up to 4–5 orders of magnitude greater than for the other halides. Therefore, for applications of these nanosensors in cells or other physiological samples, these anions would not act as interfering ions.

Application in simulated physiological media

The utility of the chloride sensitive QDs–MPA–lucigenin nanoparticles was assessed in the determination of chloride in simulated physiological samples with similar composition to the intracellular environment. The samples, taken from Dulbecco's Modified Eagle's Medium (DMEM D-6171, Sigma), contained different inorganic salts, amino acids, vitamins, glucose, and other cell components, but at higher concentration than the real intracellular levels. Dilutions of this solution were made in phosphate buffer at pH 7, achieving samples with different chloride concentrations. Further samples were prepared by spiking a 1 : 10 diluted solution of the commercial solution, with known amounts of chloride ion at four levels of concentrations. The measured luminescence signal of the QDs was used to obtain the chloride concentration from a calibration curve prepared in phosphate buffer solution. The results summarized in Table 2 show good agreement between experimental and actual values for chloride ion concentration, indicating the potential utility of the proposed QD-based nanosensors in physiological samples.

Table 2 Applications of QD620–MPA–lucigenin conjugate to chloride ion determination in samples with simulated physiological medium

Sample	Cl^- concentration actual/mM	Cl^- concentration found ± SD[a]/mM
Diluted samples DMEM D-6171	5.25	4.78 ± 0.69
	10.50	8.64 ± 1.31
	15.75	18.73 ± 2.47
Cl^- spiked samples DMEM D-6171	10.25	9.21 ± 0.44
	15.25	13.01 ± 0.49
	30.25	24.33 ± 2.19
	55.25	61.57 ± 8.67

[a] Average of three determinations ± standard deviation.

Choice of fluorescent wavelength

Fig. 4 and 5 showed that lucigenin quenches the QD fluorescence for different populations of QDs, suggesting that an additional feature of the QD–MPA–lucigenin conjugate is that the assay wavelength for chloride can be chosen. Indeed, it is based on the emission wavelength of the QD and thus not restricted to the lucigenin emission wavelength. Nearly equivalent Cl^- sensitive QDs can be constructed across a broad wavelength range, so that wavelength can potentially be selected according to instrumental convenience or to avoid background fluorescence in the sample. Fig. 9 records the chloride response for QD–MPA–lucigenin conjugate suspensions with emission wavelengths 500, 540 and 620 nm.

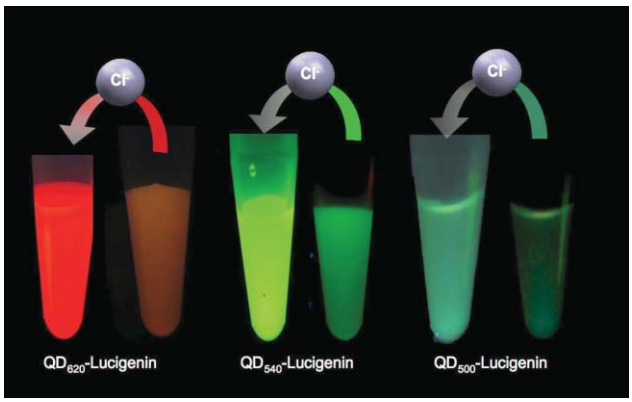

Fig. 9 Visual demonstration of Cl^- response for 3 different populations of QD–MPA–lucigenin in aqueous solution, showing how the wavelength for [Cl^-] can be chosen according to the QD selected.

Conclusions

We have demonstrated that CdSe–ZnS core–shell QD nanoparticles can efficiently interact with lucigenin (an acridinium dication) upon radiation, in a short-range (~2 nm) exchange process, producing changes in the luminescence spectrum. To demonstrate this, a simple QD–MPA–lucigenin ionic conjugate was easily achieved by electrostatic interaction through negative charged QDs and the positive charge of lucigenin.

Charge transfer between the QD and lucigenin producing the radical cation could result in reversible quenching through further fast charge transfer from the radical cation to the QD valence band. Chemiluminescent degradation of the lucigenin radical cation in competition with this QD quenching could not be found, but this doesn't rule out the charge transfer mechanism for the fluorescence quenching, since CL is likely to be slow compared with the $Luc^{+\bullet}$ to QD electron transfer. On the other hand, SOC, with or without CT, resulting in mutual quenching of the lucigenin and QD is also a likely mechanism.

In another study (unpublished results), the introduction of lucigenin modified QDs at a planar gold surface under surface plasmon excitation, showed that QD bleaching could be achieved. This would point to irreversible CT from the QD in the presence of lucigenin, consistent with $Luc^{+\bullet}$ CT-pathway mechanism. However further work is still required to provide unambiguous evidence about the CT and the dominant quenching pathway.

Since lucigenin is a broadly employed chloride ionophore, the QD–lucigenin offers a good system to investigate chloride sensitivity. The quenching of QDs can be reversed by exposure of the lucigenin–QDs to chloride ion, probably creating a competitive SOC pathway for the lucigenin quenching, thus 'turning on' the emission of the QD nanoparticles. Furthermore, a considerable asset of these lucigenin–QDs, is the ability to select the emission wavelength according to choice of QD, thereby, allowing overlap with other signals and resolution against background fluorescence to be tuned.

The suitability of these ion-sensitive QDs for the determination of chloride in physiological media was also demonstrated. If the principle was also to be used in intracellular measurement, additional issues of stability and toxicity arise. For the lucigenin–QDs sequestration of the arcidinium compounds by cellular components has been reported by others,[23,24] but in this instance we find the lucigenin–QDs complex to be stable during measurement in samples taken from Dulbecco's Modified Eagle's Medium. These samples contain many cell components. Nevertheless, an electrostatic conjugation between the lucigenin and the QD would be susceptible to cleavage and for intracellular measurements, this issue has to be addressed. In our case, issues of stability and toxicity are being considered through the design of core–shell particles. In this instance the QDs are trapped within an outer matrix. A Cl^- permeable shell can then encapsulate the ion-sensitive QD. Further applications showing that such modified QDs can be used as nanosensors for studying ion concentrations associated with measurements for cells and microorganisms, will be reported by us later.

In addition, this work provides a general framework for the creation of a new type of fluorescent probe for the detection of different analytes in physiological samples based on their redox properties or excited energy state. Although the use of QD–electron-acceptor conjugates for this purpose remains to be established, this work opens a new field of research that may lead to the development of redox sensitive probes.

Acknowledgements

The authors acknowledge support from the BBSRC (BBD0013071), the Newton Trust, Cambridge and to the Ministerio de Educación y Ciencia de España for a postdoctoral Fellowship awarded to M. J. Ruedas-Rama.

References

1 F. K. Wygladacz and E. Bakker, *Anal. Chim. Acta*, 2005, **532**, 61–69.
2 S. Peper, A. Ceresa, Y. Qin and E. Bakker, *Anal. Chim. Acta*, 2003, **500**, 127–136.
3 M. G. Brasuel, T. J. Miller, R. Kopelman and M. A. Philbert, *Analyst*, 2003, **128**, 1262–1267.
4 M. Brausel, R. Kopelman, T. J. Miller, R. Tjalkens and M. A. Philbert, *Anal. Chem.*, 2001, **73**, 2221–2228.
5 M. J. Ruedas-Rama and E. A. H. Hall, *Analyst*, 2006, **131**, 1282–1291.
6 L. F. Capitan-Vallvey, E. A. Guerrero, C. B. Merelo and M. D. F. Ramos, *Anal. Bioanal. Chem.*, 2004, **380**, 563–569.
7 B. T. T. Lan and K. Toth, *Anal. Sci.*, 1998, **14**, 191–197.
8 H. A. Badr and M. E. Mayerhoff, *Anal. Chem.*, 2005, **77**, 6719–6728.
9 P. Alivisatos, *Science*, 1996, **271**, 933–937.
10 B. Murray, D. J. Norris and M. G. Bawendi, *J. Am. Chem. Soc.*, 1993, **115**, 8706–8715.
11 M. J. Ruedas-Rama, X. Wang and E. A. H. Hall, *Chem. Commun.*, 2007, 1544–1546.
12 Y. Chen and Z. Rosenzweig, *Anal. Chem.*, 2002, **74**, 5132–5138.
13 W. J. Jin, J. M. Costa-Fernández, R. Pereiro and A. Sanz-Medel, *Anal. Chim. Acta*, 2004, **522**, 1–8.
14 K. M. Gattás-Asfura and R. M. Leblanc, *Chem. Commun.*, 2003, 2684–2685.
15 C. Y. Chen, C. T. Cheng, C. W. Lai, P. W. Wu, K. C. Wu, P. T. Chou, Y. H. Chou and H. T. Chiu, *Chem. Commun.*, 2006, 263–265.
16 M. Tomasulo, I. Yildiz and F. Raymo, *J. Phys. Chem. B*, 2006, **110**, 3853–3855.
17 B. O'Regan and M. Graetzel, *Nature*, 1991, **353**, 737–740.
18 N. C. Greenhan, X. Peng and A. P. Alivisatos, *Phys. Rev. B*, 1996, **54**, 17628–17637.
19 S. J. Clarke, C. A. Hollmann, Z. Zhang, D. Suffern, S. E. Bradforth, N. M. Dimitrijevic, W. G. Minarik and J. L. Nadeau, *Nat. Mater.*, 2006, **5**, 409–417.
20 C. Landes, C. Burda, M. Braun and M. A. El-Sayed, *J. Phys. Chem. B*, 2001, **105**, 2981–2986.
21 D. Suffern, S. J. Clarke, C. A. Hollmann, D. Bahcheli, S. E. Bradforth and J. L. Nadeau, Labeling of subcellular redox potential with dopamine-conjugated quantum dots, *Proc. SPIE*, 2006, vol. 6096.
22 M. G. Sandros, D. Gao and D. E. Benson, *J. Am. Chem. Soc.*, 2005, **127**, 12198–12199.
23 I. Yildiz and F. M. Raymo, *J. Mater. Chem.*, 2006, **16**, 1118–1120.
24 I. Yildiz, M. Tomasulo and F. M. Raymo, *Proc. Natl. Acad. Sci. U. S. A.*, 2006, **103**, 11457–11460.
25 K. Palaniappan, C. Xue, G. Arumugam, S. A. Hackney and J. Liu, *Chem. Mater.*, 2006, **18**, 1275–1280.
26 C. Burda, T. C. Green, S. Link and M. A. El-Sayed, *J. Phys. Chem. B*, 1999, **103**, 1783–1788.
27 C. Huber, C. Krause, T. Werner and O. Wolfbeis, *Microchim. Acta*, 2003, **142**, 245–253.
28 C. Huber, I. Klimant, C. Krause, T. Werner, T. Mayr and O. S. Wolfbeis, *J. Anal. Chem.*, 2000, **368**, 196–202.
29 C. Huber, K. Fähnrich, C. Krause and T. Werner, *J. Photochem. Photobiol., A*, 1999, **128**, 111–120.
30 W. C. W. Chan and S. Nie, *Science*, 1998, **281**, 2016–2018.
31 G. P. Mitchell, C. A. Morkin and R. L. Letsinger, *J. Am. Chem. Soc.*, 1999, **121**, 8122–8123.
32 F. Patolsky, R. Gill, Y. Weizmann, T. Mokari, U. Banin and I. Willner, *J. Am. Chem. Soc.*, 2003, **125**, 13918–13919.
33 H. T. Uyeda, I. L. Medintz, J. K. Jaiswal, S. M. Simon and H. Mattoussi, *J. Am. Chem. Soc.*, 2005, **127**, 3870–3878.
34 S. F. Wuister, I. Swart, F. van Driel, S. G. Hickey and C. de Mello Donegá, *Nano Lett.*, 2003, **3**, 503–507.
35 H. Mattoussi, J. M. Mauro, E. R. Goldman, G. P. Anderson, V. C. Sundar, F. V. Mikulec and M. G. Bawendi, *J. Am. Chem. Soc.*, 2000, **122**, 12142–12150.
36 X. Ji, J. Zheng, J. Xu, V. K. Rastogi, T. C. Cheng, J. J. DeFrank and R. M. Leblanc, *J. Phys. Chem. B*, 2005, **109**, 3793–3799.
37 C. A. Constantine, K. M. Gattás-Asfura, S. V. Mello, G. Crespo, V. Rastogi, T.-C. Cheng, J. J. DeFrank and R. M. Leblanc, *J. Phys. Chem. B*, 2003, **107**, 13762–13764.
38 R. E. Heikka, D. W. Deamer and D. G. Cornwell, *J. Lipid Res.*, 1970, **11**, 195–200.
39 Q. R. Huang, P. L. Dubin, C. N. Moorefield and G. R. Newkome, *J. Phys. Chem. B*, 2000, **104**, 898–904.
40 S. H. Behrens, D. I. Christl, R. Emmerzael, P. Schurtenberger and M. Borkovec, *Langmuir*, 2000, **16**, 2566–2575.
41 S. Budavari, *Merck Index*, Merck Research Labs, Whitehouse Station, NJ, 12th edn, 1996.
42 J. R. Kanicky, A. F. Poniatowski, N. R. Mehta and D. O. Shah, *Langmuir*, 2000, **16**, 172–177.
43 J. R. Kanicky and D. O. Shah, *Langmuir*, 2003, **19**, 2034–2038.
44 J. C. Scaiano, M. Laferrière, R. E. Galian, V. Maurel and P. Billone, *Phys. Status Solidi*, 2006, **203**, 1337–1343.

45 R. Clapp, I. L. Medintz, J. M. Mauro, B. R. Fisher, M. G. Bawendi and H. Mattoussi, *J. Am. Chem. Soc.*, 2004, **126**, 301–310.
46 J. Z. Guo and H. Cui, *J. Phys. Chem. C*, 2007, **111**, 12254–12259.
47 X. Gao, W. C. W. Chan and S. Nie, *J. Biomed. Opt.*, 2002, **7**, 532–537.
48 M. Idowu, J.-Y. Chen and T. Nyokong, *New J. Chem.*, 2008, **32**, 290–296.
49 R. I. Cukier, *J. Am. Chem. Soc.*, 1985, **107**, 4115–4117.
50 IUPAC, *Spectrochim. Acta, Part B*, 1976, **33**, 242.
51 ACS Committee on Environmental Improvement, *Anal. Chem.*, 1980, **52**, 2242.

